

RESEARCH ARTICLE

Numerical Solution of Integral Equations by using Discrete GHM Multi-wavelet

* Archit Yajnik¹, Rustam Ali¹

¹Department of Mathematics, Sikkim Manipal University, India.

Received-26 October 2015, Revised-20 November 2015, Accepted-21 November 2015, Published-27 November 2015

ABSTRACT

In this paper, numerical solution based on discrete GHM multi-wavelets is presented for solving the Fredholm integral equations of second kind. There is hardly any article available in the literature in which the integral equations are numerically solved using discrete Geronimo-Hardin-Massopust (GHM) multi-wavelet. The localization property, robustness and other features of wavelets are essential for solving integral equations efficiently. A number of examples are demonstrated to justify the applicability of the method. In GHM multi-wavelets, the values of scaling and wavelet functions are calculated only at $t = 0, 0.5$ and 1 . The numerical solution obtained by the present approach is compared with the traditional Quadrature method. It is observed that the present approach is more accurate and computationally efficient when compared to Quadrature method.

Keywords: GHM Multi-wavelet, Fredholm integral equations, Quadrature Method, Function Approximation, Scaling.

1. INTRODUCTION

The properties of localization in frequency as well as space in wavelet function make it a very convenient and powerful tool for various applications like image approximation, signal processing, solution of differential and integral equations etc. [1]-[5]. The main advantage of the wavelet analysis is its accuracy and ability to transform complex problems into a system of algebraic equations and thus making it computationally feasible.

There have been a number of investigations in order to use wavelet expansions for the numerical computation of solutions for integral equations [6]-[11]. But all of them use the continuous scaling and wavelet functions which make the procedure computationally very costly whereas the present approach uses only three values of GHM multi-wavelets to obtain the solution which makes the task very lucid with compromise to the accuracy of the solution. The description of the GHM is introduced in [1] where the signal $f(t)$ is being calculated at half integers. However, the continuous-time

function $f(t)$ belong to the scale-limited subspace V_0 generated by translates of the GHM scaling functions. This means that $f(t)$ is a linear combination of translates of the functions $\phi_1(t)$ and $\phi_2(t)$ as shown in section 2. In the case of continuous domain the problem becomes computationally very costly because the original construction of the GHM basis, using fractal interpolation functions, is quite complicated.

The paper is divided into five sections. After the introduction in section 1, the preliminaries of the GHM multi-wavelet is presented in section 2. The approach presented in section 3 describes the GHM based numerical solution of integral equations. Four integral equations are illustrated in section 4, based on the present technique and the solutions are compared with the traditional quadrature method [13]. The paper is concluded in section 5 followed by the references.

2. GHM MULTI-WAVELETS

GHM multi-wavelets have two scaling and wavelet functions. For notational

*Corresponding author. Tel.: +919635319656

Email address: archit.yajnik@gmail.com (A.Yajnik)

Double blind peer review under responsibility of DJ Publications

<http://dx.doi.org/10.18831/djmaths.org/2015011003>

2455-362X © 2016 DJ Publications by Dedicated Juncture Researcher's Association. This is an open access article under the CC BY-NC-ND license (<http://creativecommons.org/licenses/by-nc-nd/4.0/>).

convenience, the set of scaling functions can be written using the vector notation $\Phi(t) = [\phi_1(t), \phi_2(t)]^T$, where $\Phi(t)$ is called the multiscaling function. Likewise, the multi-wavelet function is defined from the set of wavelet functions as $\Psi(t) = \Psi_1(t) + \Psi_2(t)$. The multi-wavelet two-scale equations resemble those for scalar wavelets.

$$\Phi(t) = \sqrt{2} \sum_{k=-\infty}^{\infty} H_k \Phi(2t - k) \quad (2.1)$$

$$\Psi(t) = \sqrt{2} \sum_{k=-\infty}^{\infty} G_k \Psi(2t - k) \quad (2.2)$$

Note, however, that $\{H_k\}$ and $\{G_k\}$ are matrix filters, i.e., H_k and G_k are $r \times r$ matrices for each integer k . The matrix elements in these filters provide more degrees of freedom than a traditional scalar wavelet. These extra degrees of freedom can be used to incorporate useful properties into the multi-wavelet filters, such as orthogonality, symmetry, and high order of approximation [10], [12]. One famous multi-wavelet filter is the GHM filter proposed by Geronimo, Hardian, and Massopust [5]. The GHM basis offers a combination of orthogonality, symmetry, and compact support which cannot be achieved by any scalar wavelet [6], [11].

$$H_0 = \begin{bmatrix} \frac{3}{5\sqrt{2}} & \frac{4}{5} \\ -\frac{1}{20} & \frac{3}{10\sqrt{2}} \end{bmatrix}, H_1 = \begin{bmatrix} \frac{3}{5\sqrt{2}} & 0 \\ \frac{9}{20} & \frac{1}{\sqrt{2}} \end{bmatrix},$$

$$H_2 = \begin{bmatrix} 0 & 0 \\ \frac{9}{20} & \frac{3}{10\sqrt{2}} \end{bmatrix}, H_3 = \begin{bmatrix} 0 & 0 \\ -\frac{1}{20} & 0 \end{bmatrix}$$

$$G_0 = \begin{bmatrix} -\frac{1}{20} & \frac{3}{10\sqrt{2}} \\ \frac{1}{10\sqrt{2}} & \frac{3}{10} \end{bmatrix}, G_1 = \begin{bmatrix} \frac{9}{20} & \frac{1}{\sqrt{2}} \\ -\frac{9}{10\sqrt{2}} & 0 \end{bmatrix},$$

$$G_2 = \begin{bmatrix} \frac{9}{20} & \frac{3}{10\sqrt{2}} \\ \frac{9}{10\sqrt{2}} & -\frac{3}{10} \end{bmatrix}, G_3 = \begin{bmatrix} -\frac{1}{20} & 0 \\ -\frac{1}{10\sqrt{2}} & 0 \end{bmatrix}$$

Iteration scheme described by equation (2.1) and (2.2) is used to draw the scaling and wavelet function for the GHM multi-wavelets. However, in this case there are two scaling functions and two wavelets functions starting from two box functions as shown in figure B1. Figure B2 shows the GHM pair of multiwavelets.

3. FUNCTION APPROXIMATION

According to equations (2.1) and (2.2) the GHM two scaling and wavelet functions

satisfy the following two scale dilation equations:

$$\begin{bmatrix} \phi_1(t) \\ \phi_2(t) \end{bmatrix} = \sqrt{2} \sum_k H_k \begin{bmatrix} \phi_1(2t - k) \\ \phi_2(2t - k) \end{bmatrix} \quad (3.1)$$

$$\begin{bmatrix} \Psi_1(t) \\ \Psi_2(t) \end{bmatrix} = \sqrt{2} \sum_k G_k \begin{bmatrix} \phi_1(2t - k) \\ \phi_2(2t - k) \end{bmatrix} \quad (3.2)$$

From figure B1, $\phi_1(t)$ vanishes at all integer points. $\phi_2(t)$ is nonzero only at integer 1. Incorporating this information and taking $t = 0$ in equation (3.1) and (3.2), we get

$$\begin{bmatrix} \phi_1(t) \\ \phi_2(t) \end{bmatrix} = \begin{bmatrix} 0 \\ 0 \end{bmatrix} = \begin{bmatrix} \Psi_1(0) \\ \Psi_2(0) \end{bmatrix} \quad (3.3)$$

Similarly using equation (3.1) and (3.2) at $t = \frac{1}{2}$,

$$\begin{bmatrix} \phi_1(0.5) \\ \phi_2(0.5) \end{bmatrix} = \sqrt{2} \begin{bmatrix} H_0 \begin{bmatrix} \phi_1(1) \\ \phi_2(1) \end{bmatrix} + H_1 \begin{bmatrix} \phi_1(0) \\ \phi_2(0) \end{bmatrix} \end{bmatrix},$$

we get,
$$\begin{bmatrix} \phi_1(0.5) \\ \phi_2(0.5) \end{bmatrix} = \begin{bmatrix} \frac{4\sqrt{6}}{5} \\ -\frac{3\sqrt{3}}{10} \end{bmatrix} \quad (3.4)$$

$$\begin{bmatrix} \Psi_1(0.5) \\ \Psi_1(0.5) \end{bmatrix} = \sqrt{2} \begin{bmatrix} G_0 \begin{bmatrix} \phi_1(1) \\ \phi_2(1) \end{bmatrix} + G_1 \begin{bmatrix} \phi_1(0) \\ \phi_2(0) \end{bmatrix} \end{bmatrix},$$

we get,
$$\begin{bmatrix} \Psi_1(0.5) \\ \Psi_1(0.5) \end{bmatrix} = \begin{bmatrix} -\frac{3\sqrt{3}}{10} \\ \frac{3\sqrt{6}}{10} \end{bmatrix} \quad (3.5)$$

Applying the same procedure at $t = 1$,

$$\begin{bmatrix} \phi_1(1) \\ \phi_2(1) \end{bmatrix} = \begin{bmatrix} \sqrt{3} \\ 0 \end{bmatrix}, \begin{bmatrix} \Psi_1(1) \\ \Psi_2(1) \end{bmatrix} = \begin{bmatrix} -1.7321 \\ 0.00000 \end{bmatrix} \quad (3.6)$$

We consider the integral equation

$$y(x) + \int_0^1 K(x, t)y(t)dt = g(x), \quad 0 \leq x \leq 1 \quad (3.7)$$

where $y(x)$ is an unknown function to be determined and $g(x)$ is a known function. For the sake of simplicity denote $\Psi_1 = \Psi^1$ and $\Psi_2 = \Psi^2$ in the following procedure. To find an approximate solution of [9] we approximate $y(x)$ using GHM multi-wavelet in the interval $[0,1]$ as

$$y(x) = C_1 \phi_1(x) + C_2 \phi_2(x) + \sum_{j=1}^2 \sum_{k=0}^M \sum_{n=0}^{2^k-1} C_{k,n}^j \Psi_{k,n}^j = C \chi^T(x) \quad (3.8)$$

where C and $\chi(x)$ are matrices given

by

$$C = [c_0, c_{0,0}^1, \dots, c_{M,(2^{M-1})}^1, c_{0,0}^2, \dots, c_{M,(2^{M-1})}^2]$$

and

$$\chi(x) = [\phi_1, \phi_1, \Psi_{0,0}^1, \dots, \Psi_{M,(2^{M-1})}^1, \Psi_{0,0}^2, \dots, \Psi_{M,(2^{M-1})}^2]^T$$

Substituting equation (3.8) in (3.7) we obtain

$$C\chi^T(x) + \int_0^1 K(x,t)C\chi^T(t)dt = g(x)$$

Putting $x = x_i$, x_i 's being suitably chosen by dividing $[0,1]$ into n equal segments, we obtain the system.

$$CX = B \tag{3.9}$$

where

$$X = (a_{i,j})_{n+1,2^{(M+2)}} = \left[\begin{array}{c} \chi^T(x_i) \\ + \int_0^1 K(x_i,t)\chi^T(t)dt \end{array} \right]$$

and $B = [g(x_i)]_{n+1}$.

By approximating the integral $\int_0^1 K(x_i,t)\chi^T(t)dt$ numerically, we can easily compute the matrix X . Solving the system (3.9) we can obtain the coefficient matrix C which ultimately helps in determining the solution $f(x)$.

4. ILLUSTRATIVE EXAMPLES

The interval $x = [0, 1]$ is divided into 2 equal parts. Hence $x_0 = 0, x_1 = 0.5$ and $x_2 = 1$. Taking $M = 1$ in equation (3.8), we get a basis vector.

$$\chi(x) = [\phi_1, \phi_2, \Psi_{0,0}^0, \Psi_{1,0}^0, \Psi_{1,1}^0, \Psi_{0,0}^0, \Psi_{1,0}^0, \Psi_{1,1}^0]^T$$

As shown in equations (3.3), (3.4), (3.5) and (3.6) in section 3, $\chi(x)$ is being calculated at each $x = x_i$ where $i = 0, 1, 2$.

$$\chi(0) = [0.000000001 \ 0, 0, 0, 0, 0, 0, 0]^T$$

$$\chi(0) = [1.959, 6 - 0.519, 6 - 0.519, 6 - 2.4495, 0 \ 0.734, 8 \ 0, \ 0]^T$$

$$\chi(1) = [0, \ 1.732, 1 - 1.732 \ 0, -2.4495, 0, \ 0, \ 0]^T$$

Thus, the matrix X shown in equation (3.9) will be of the size 3×8 and correspondingly the coefficient matrix C will be of the size 8×1 . Finally, substituting the value of C in equation (3.8), the solution $y(x) = \widehat{y}_1$ is attained. Kernals used in the following Illustrations I and III are linear whereas II and IV are nonlinear.

[I] Consider the integral equation

$$y(x) - \int_0^1 (t+x)y(y)dt = \frac{3}{2}x - \frac{5}{6}$$

[II] Consider,

$$y(x) + \int_0^1 \sin(tx) y(t)dt = 1$$

[III] Consider,

$$y(x) + \int_0^1 (t+x)y(y)dt = 1$$

[IV] Consider,

$$y(x) - \int_0^1 (t^2 + x^2)y(y)dt = 1$$

5. CONCLUSION

A novel technique of using discrete GHM multi-wavelets to obtain the numerical solution of Fredholm integral equations of second kind is presented in this article. Since the close form of scaling and wavelet functions of GHM is not available, the values of ϕ_1, ϕ_2, ψ_1 and ψ_2 are obtained only at three places viz. $t = 0, 0.5$ and 1 . It makes the present approach based on GHM, computationally very less expensive as compared to other existing approaches which are based on continuous wavelet functions [3, 5, 11]. As shown in section IV, it is observed that for linear kernel (Illustration I and III), both the approaches viz. GHM multi-wavelet and Quadrature method gave exact solution whereas for nonlinear kernals (Illustration II and IV) GHM based approach yields better solution than the traditional quadrature method. Particularly in illustration II, where the kernel is a sine function, quadrature method completely fails while present technique yields significant accuracy as shown in table A3. Tables A1, A2, A3 and A4 provide the details. The accuracy may further be ameliorated by calculating more values of the GHM multi-wavelets or by enhancing the value of M .

REFERENCES

- [1] V.Strela, P.N.Heller, G.Strang, P.Topiwala and C.Heil, The

- Application of Multiwavelet Filter Banks to Image Processing, IEEE Transaction on Image Processing, Vol. 8, 1995, pp. 548-563.
- [2] M.Devi, S.R.Verma and M.P.Singh, Solving Differential Equations of Second Order using Quadratic Legendre Multi-wavelets (QLMW) with Operational Matrix of Integration, International Journal of Computer Applications, Vol. 75, No. 15, 2013, pp. 43-49.
<http://dx.doi.org/10.5120/13190-0912>
- [3] Yajnik, Wavelet Analysis and its Applications-An Introduction, Narosa Publishing House, New Delhi, India, 2013.
- [4] www.uni-due.de/~hm0029/pdfs/lillehammer.pdf
- [5] Lokenath Debnath, Wavelet Transforms and Their Applications, Birkhauser, Boston, USA, 2002,
<http://dx.doi.org/10.1007/978-1-4612-0097-0>
- [6] E.Hesameddini and S.Shekarpez, Wavelet Solutions of the Second Painleve Equation, Iranian Journal of Science Technology, 2011, pp. 287-291.
- [7] J.Liandratt, V.Perrier and Ph.Tchamitchian, Numerical Resolution of Nonlinear Partial Differential Equations using the Wavelet Approach, Wavelets and their Applications, 1992.
- [8] R.L.Schult and H.W.Wyld, Using Wavelets to Solve the Burgers Equation-A comparative study, Physical Review A, Vol. 46, No. 12, 1992, pp. 12,
<http://dx.doi.org/10.1103/PhysRevA.46.7953>.
- [9] A.S.Yakovlev, Wavelets as a Galerkin basis, Department of Computational Physics, St. Petersburg State University, 1994.
- [10] R.K.Singh, A.Pathak and B.N.Mandal, Numerical Solution of Linear Fredholm and Volterra Integral Equations of the second kind by using Quadratic Legendre Multi-Wavelets
- [11] En-Bing Lin and Yousef Al-Jarrah, Wavelet Based Methods for Numerical Solutions of Two Dimensional Integral Equations, Mathematics Aeterna, Vol. 4, No. 8, 2014, pp. 839-853.
- [12] Hamid Soltanian-Zadeh, Farshid Rafiee-Rad and D.Siamak Pourabdollah-Nejad, Comparison of Multiwavelet, Wavelet, Haralick and Shape Features for Microcalcification Classification in Mammograms, Pattern Recognition, Vol. 37, No. 10, 2004, pp. 1973-1986,
<http://dx.doi.org/10.1016/j.patcog.2003.03.001>
- [13] S.S.Sastry, Introductory Methods of Numerical Analysis, PHI, New Delhi, India, 2013.

APPENDIX A

Table A1.Comparison of solution

x	\widehat{y}_1 (Solution using GHM wavelet)	\widehat{y}_2 (Solution using Quadrature method)	Exact Solution $y(x) = 1 - x$
0	-1	-1	-1
0.5	-0.5	-0.5	-0.5
1	0	0	0

Table A2.Comparison of solution

x	\widehat{y}_1 (Solution using GHM wavelet)	\widehat{y}_2 (Solution using Quadrature method)	Exact Solution $y(x) = \frac{x}{(x+1)-\cos x}$
0	1	1	1
0.5	0.8139	0.72634	0.80
1	0.6489	0.51965	0.6850

Table A3.Comparison of solution

x	\widehat{y}_1 (Solution using GHM wavelet)	\widehat{y}_2 (Solution using Quadrature method)	Exact Solution $y(x) = \frac{18}{23} - \frac{12}{23}x$
0	0.7826	0.7836	0.7826
0.5	0.5217	0.5217	0.5217
1	0.2609	0.2608	0.2609

Table A4.Comparison of solution

x	\widehat{y}_1 (Solution using GHM wavelet)	\widehat{y}_2 (Solution using Quadrature method)	Exact Solution $y(x) = \frac{45}{11}x^2 + \frac{30}{11}$
0	2.8235	2.8235	2.7273
0.5	3.8824	3.8824	3.75
1	7.0588	7.0588	6.818

APPENDIX B

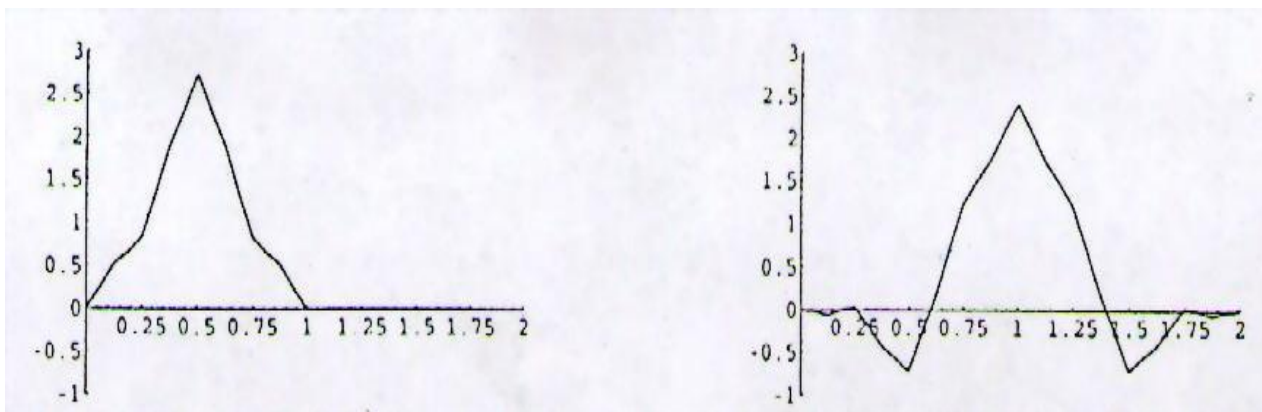


Figure B1.GHM pair of scaling functions

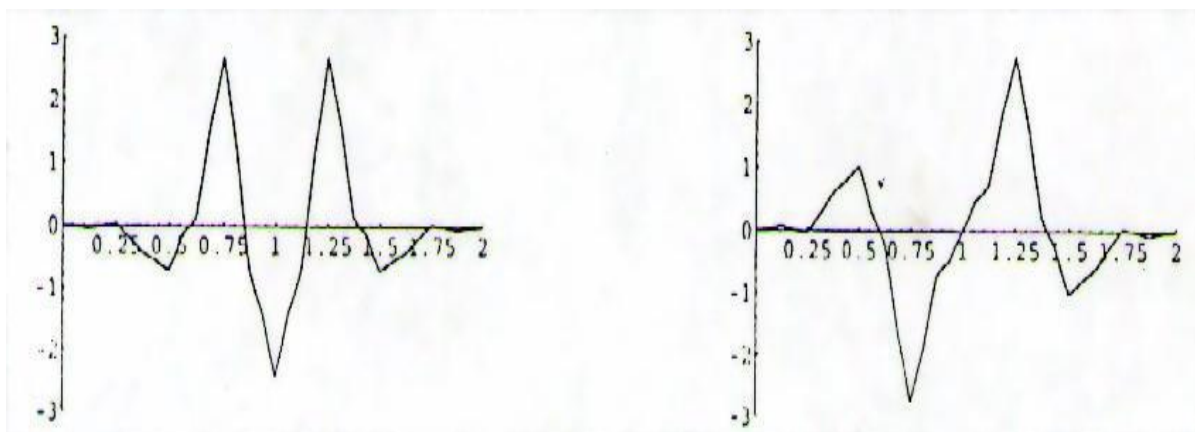


Figure B2.GHM pair of multiwavelets.